2014

Diversity Order and Coding Gain of General-Order Rectangular QAM in MIMO Relay With TAS/MRC in Nakagami-*m* Fading

Won Mee Jang
University of Nebraska - Lincoln, wjang1@unl.edu

Pages: 3157 - 3166, DOI: 10.1109/TVT.2014.2301022

Diversity Order and Coding Gain of General-Order Rectangular QAM in MIMO Relay With TAS/MRC in Nakagami-m Fading

Won Mee Jang

***Abstract*—Recently, multiple-input–multiple-output (MIMO) relay networks have been an active area of research, particularly with combining single transmit antenna selection (TAS) and receiver maximal ratio combining (MRC). Moreover, general-order rectangular quadrature amplitude modulation (QAM) has received much attention for its high spectral efficiency and flexible modulation scheme. However, the analytical performance of general-order rectangular QAM has not been found in the literature for MIMO relay with TAS/MRC in Nakagami-m fading channels in spite of its practical usefulness. In addition, the analytical performance of general-order rectangular QAM often comes with enormous computational complexity. Therefore, it is hardly possible to understand the analytical solution unless the symbol error probability (SEP) is plotted graphically. In this paper, we present the SEP of general-order rectangular QAM in a MIMO relay with TAS/MRC using the sampling property of the delta impulse function. The SEP of MIMO relay networks is shown in terms of diversity order and coding gain. The proposed sampling method can also significantly reduce the computational complexity of the SEP of general-order rectangular QAM.**

***Index Terms*—General-order rectangular quadrature amplitude modulation (QAM), multiple-input–multiple-output (MIMO) relay, Nakagami-m, sampling, transmit antenna selection/maximal ratio combining (TAS/MRC).**

I. Introduction

THE bit error probability (BEP) by sampling in various fading channels and cooperative diversity networks was introduced in [1]–[3]. The proposed method reduces an integration of the Q-function with a fading probability density function (pdf) into a simple sampling using the sampling property of a delta function. The sampling BEP can provide a simple solution by eliminating the moment generating function (MGF) approach, commonly employed in spite of its computational difficulties, for finding the system performance in fading channels. The proposed sampling approach can also find the coding gain and diversity order when it is difficult to obtain due to complexities of the performance expression. Recently, general-order rectangular quadrature amplitude modulation (QAM) [4] has received much attention for its high spectral efficiency and flexible implementation. Moreover, single transmit antenna selection (TAS) with maximal ratio combining (MRC) is shown to achieve full transmit and receive diversity in point-to-point communications with low complexity [5]. In this paper, we present a simple closed-form symbol error probability (SEP) of general-order rectangular QAM in multiple-input–multiple-output (MIMO) systems and MIMO relay networks with TAS/MRC in Nakagami-m fading channels using a sampling method. The proposed sampling SEP is crucial since the exact SEP of general-order rectangular QAM in MIMO relay networks with TAS/MRC is not available in the literature to the best of the author's knowledge. Moreover, the result can be reduced to square M-QAM in MIMO [6] or MIMO relay networks [7] to provide a much simpler solution of the SEP. In fact, the SEP of QAM with MIMO, which is currently available in the literature, comes with enormous computational complexity and makes it extremely difficult to comprehend the effect of system parameters such as fading characteristics or the number of antennas employed. In fact, the key system parameters are literally buried in the hypergeometric functions. On the other hand, the contribution of each system parameter is transparent in the sampling SEP, which is critical in the design and validation of MIMO systems.

We extend the result in [3] to practical scenarios of interest such as MIMO or MIMO relay with TAS/MRC. The major challenges for the extension arise from the incomplete gamma function in the TAS/MRC fading pdf. In the sampling approach, the sampling function should be more similar to a delta impulse function than the sampled function in [12]. To make this happen, we need to dissect the incomplete gamma function. The detailed process is presented in the Appendix. In particular, we present a simple closed-form solution unlike the SEP of QAM with MIMO in the literature, which remains in an integral form with an integrand of the MGF in [7] or comes with the confluent hypergeometric functions in [6] and [8]. The SEP is available only for an integer fading parameter m for general-order rectangular QAM in single-input–single-output (SISO) [4], [9], or square M-QAM in MIMO relay networks with TAS/MRC [7]. On the other hand, the performance of M-QAM was obtained in Nakagami-m fading channels for real fading parameter m in SISO [10] and MIMO with TAS/MRC [6]. The performance of rectangular QAM with combined arbitrary TAS and receive MRC with real fading parameter was analyzed using the confluent hypergeometric function and the Lauricella hypergeometric function in [11].

Manuscript received August 21, 2013; revised November 16, 2013; accepted January 15, 2014. Date of publication January 16, 2014; date of current version September 11, 2014. The review of this paper was coordinated by Dr. T. Taniguchi.

The author is with Department of Computer and Electronics Engineering, University of Nebraska–Lincoln, Lincoln, NE 68182-0572 USA (e-mail: wjang1@unl.edu).

Color versions of one or more of the figures in this paper are available online at http://ieeexplore.ieee.org.

Digital Object Identifier 10.1109/TVT.2014.2301022

Our proposed SEP can be established for general-order rectangular QAM in MIMO relay networks with TAS/MRC for arbitrary real-valued fading parameter m. The proposed sampling SEP is simple and easy to compute and yet provides crucial information for the system performance such as diversity order and coding gain. The diversity order and coding gain are currently available only in square M-QAM with MIMO or MIMO networks, and come with enormous computational complexity due to the MGF approach employed in the evaulation. In fact, the sampling SEP of general-order rectangular QAM in MIMO precisely overlaps with simulation results for all SNRs. The corresponding asymptotic sampling SEP in MIMO relay networks in terms of coding gain and diversity order accurately represents the simulation SEP for moderate and high SNRs.

In Section II, we briefly introduce the sampling SEP. The sampling SEP of general-order rectangular QAM in MIMO with TAS/MRC is presented in Section III. The sampling SEP is extended to MIMO relay networks with distributed TAS/MRC in Section IV. Numerical results are illustrated in Section V. Section VI concludes this paper.

II. Example Sampling Bit Error Probability

The probability of a bit error of a BPSK in a flat Rayleigh fading channel can be expressed as [12]

$$P_b(r_b) = \int_0^\infty Q(\sqrt{2r_b r}) \exp\{-r\} dr \tag{1}$$

where r_b is the bit-energy-to-noise ratio, and the Q-function is defined as $Q(x) \doteq \int_x^\infty (1/\sqrt{2\pi}) \exp\{-y^2/2\} dy$. The sampling method reduces an integration of the Q-function with a fading pdf to a simple sampling. The expression of $\exp\{-r\}$ in (1) indicates the pdf of the power fluctuation in Rayleigh fading. With a change of a variable $r = t^N$, (1) can be written as

$$P_b = \int_0^\infty Q\left(\sqrt{2r_b t^N}\right) \exp\{-t^N\} N t^{N-1} dt. \tag{2}$$

Let us choose a sampling function, i.e.,

$$s(t^N) = Q\left(\sqrt{2r_b t^N}\right) N t^{N-1}. \tag{3}$$

Then, we can find the critical point using Leibnitz's differential rule [13], i.e.,

$$\frac{ds(t^N)}{dt} = -\sqrt{2r_b}\frac{N}{2} t^{\frac{N}{2}-1} \frac{1}{\sqrt{2\pi}} \exp\{-r_b t^N\} N t^{N-1} + \frac{1}{\sqrt{4\pi r_b t^N}} \exp\{-r_b t^N\} N(N-1) t^{N-2} = 0 \tag{4}$$

where we employed the Q-function approximation of $Q(x) \approx (1/\sqrt{2\pi x^2}) \exp\{-x^2/2\}$ [14]. From (4), we find the critical point $t_*^N = 1/r_b$ as N approaches infinity. Moreover

$$\frac{ds(t^N)}{dt} > 0 \quad \text{for} \quad 0 < t^N < t_*^N$$
$$\frac{ds(t^N)}{dt} < 0 \quad \text{for} \quad t^N > t_*^N \tag{5}$$

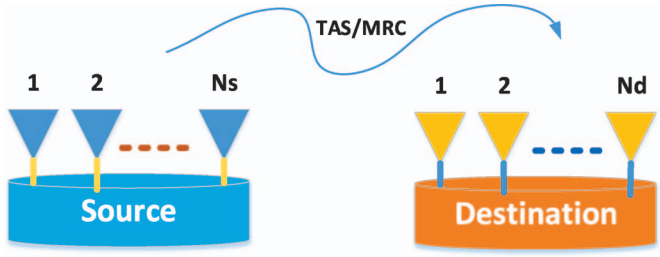

Fig. 1. N_s transmit antennas and N_d receive antennas of the MIMO system with TAS/MRC.

indicating that $s(t^N)$ is a unimodal function for $t^N > 0$. From (3), we observe that

$$\lim_{N\to\infty} s\left(t_*^N\right) = Q(\sqrt{2}) N \frac{1}{r_b} = \infty \tag{6}$$
$$\int_0^\infty s(t^N) dt = \int_0^\infty Q(\sqrt{2r_b r}) dr = \frac{1}{4r_b}. \tag{7}$$

From (5)–(7), we deduce [12]

$$\lim_{N\to\infty} s(t^N) = \frac{1}{4r_b} \delta\left(t^N - \frac{1}{r_b}\right). \tag{8}$$

Therefore, we can rewrite (2) as

$$P_b = \int_0^\infty \frac{1}{4r_b} \delta\left(t^N - \frac{1}{r_b}\right) \exp\{-t^N\} dt = \frac{1}{4r_b} \exp\left\{-\frac{1}{r_b}\right\} \tag{9}$$

and, at a high SNR, as

$$P_b \approx \frac{1}{4r_b} \tag{10}$$

which is the well-known fact of the performance of BPSK at a high SNR [15]. We denote a preimpulse function [3], i.e.,

$$g_p(r) = Q(\sqrt{2r_b r}) \tag{11}$$

and the corresponding asymptotic impulse function [12]

$$g(r) = \frac{1}{4r_b} \delta\left(r - \frac{1}{r_b}\right) \tag{12}$$

to simplify the sampling process as

$$P_b(r_b) = \int_0^\infty Q(\sqrt{2r_b r}) \exp\{-r\} dr \tag{13}$$
$$\approx \int_0^\infty \frac{1}{4r_b} \delta\left(r - \frac{1}{r_b}\right) \exp\{-r\} dr = \frac{1}{4r_b} \exp\left\{-\frac{1}{r_b}\right\}. \tag{14}$$

III. Sampling Symbol Error Probablity in Multiple-Input–Multiple-Output With Transmit Antenna Selection/Maximal Ratio Combining

Let us consider the SEP of the MIMO system with N_s transmit antennas and N_d receive antennas shown in Fig. 1.

The average symbol-energy-to-noise ratio of the general-order rectangular $M_I \times M_Q$-QAM can be written as [9]

$$\frac{E_T}{\sigma_n^2} = a^2\Omega\left(\frac{M_I^2-1}{3}\right) + b^2\Omega\left(\frac{M_Q^2-1}{3}\right) = a^2\Omega\left[\left(\frac{M_I^2-1}{3}\right) + \gamma^2\left(\frac{M_Q^2-1}{3}\right)\right] \quad (15)$$

where $a = d_I/\sigma_n$, and $b = d_Q/\sigma_n$. Symbols d_I and d_Q denote the in-phase and quadrature decision distances, respectively. σ_n^2 denotes noise power and the ratio of the quadrature to in-phase decision distance is $\gamma = b/a = d_Q/d_I$. The SEP of the general-order rectangular $M_I \times M_Q$-QAM in SISO [4], [9] can be extended to MIMO with TAS/MRC, with N_s transmit and N_d receive antennas in independent flat Nakagami-m fading channels, as

$$\begin{aligned} P(a,\, b,\, m,\, N_s,\, N_d) &= 2\left(1-\frac{1}{M_I}\right)\Psi(a,\, m,\, N_s,\, N_d) \\ &\quad + 2\left(1-\frac{1}{M_Q}\right)\Psi(b,\, m,\, N_s,\, N_d) \\ &\quad - 4\left(1-\frac{1}{M_I}\right)\left(1-\frac{1}{M_Q}\right)\Upsilon(a,\, b,\, m,\, N_s,\, N_d) \end{aligned} \quad (16)$$

where

$$\Psi(a,\, m,\, N_s,\, N_d) = \int_0^\infty Q(ar) f_r(r,\, m,\, N_s,\, N_d)dr \quad (17)$$

$$\Upsilon(a,\, b,\, m,\, N_s,\, N_d) = \int_0^\infty Q(ar)Q(br) f_r(r,\, m,\, N_s,\, N_d)dr. \quad (18)$$

In addition, the Nakagami-m fading pdf in MIMO with TAS/MRC can be expressed as [6], [16], [17]

$$f_r(r,\, m,\, N_s,\, N_d) = 2N_s\left(\frac{m}{\Omega}\right)^{mN_d}\frac{r^{2mN_d-1}}{\Gamma(mN_d)} \times \exp\left\{-\frac{m}{\Omega}r^2\right\}\left[\frac{\gamma(mN_d, \frac{m}{\Omega}r^2)}{\Gamma(mN_d)}\right]^{N_s-1} U(r) \quad (19)$$

with $U(r)$ being the unit step function, and the lower incomplete gamma function $\gamma(\alpha,\, x) = \int_0^x t^{\alpha-1}e^{-t}dt$ for $\alpha > 0$. Then, we can find the sampling SEP $P_s(a,\, b,\, m,\, N_s,\, N_d)$ replacing Ψ and Υ in (16) with Ψ_s and Υ_s, as shown in the Appendix, i.e.,

$$\begin{aligned} &\Psi_s(a,\, m,\, N_s,\, N_d) \\ &= \frac{1}{\sqrt{2\pi}a\sqrt{\frac{mN_sN_d}{K_a}}}\left(1-\exp\left\{-c_o a\sqrt{\frac{mN_sN_d}{K_a}}\right\}\right) \\ &\quad \times \frac{N_s}{\Gamma(mN_d)^{N_s}}\left(\frac{m}{\Omega}\right)^{mN_sN_d} \\ &\quad \times \left[\sum_{k=0}^{\infty}\frac{\left(\frac{m}{\Omega}\left[\frac{mN_sN_d}{K_a}\right]\right)^k}{\prod_{i=0}^{k}(mN_d+i)}\right]^{N_s-1}\frac{\Gamma(mN_sN_d)}{K_a^{mN_sN_d}} \end{aligned} \quad (20)$$

$$\begin{aligned} &\Upsilon_s(a,\, b,\, m,\, N_s,\, N_d) \\ &= \frac{1}{2\pi ab\left(\frac{mN_sN_d}{K_{ab}}\right)}\left(1-\exp\left\{-c_o a\sqrt{\frac{mN_sN_d}{K_{ab}}}\right\}\right) \\ &\quad \times \left(1-\exp\left\{-c_o b\sqrt{\frac{mN_sN_d}{K_{ab}}}\right\}\right)\left(\frac{m}{\Omega}\right)^{mN_sN_d} \\ &\quad \times \frac{N_s}{\Gamma(mN_d)^{N_s}}\left[\sum_{k=0}^{\infty}\frac{\left(\frac{m}{\Omega}\left[\frac{mN_sN_d}{K_{ab}}\right]\right)^k}{\prod_{i=0}^{k}(mN_d+i)}\right]^{N_s-1}\frac{\Gamma(mN_sN_d)}{K_{ab}^{mN_sN_d}}. \end{aligned} \quad (21)$$

The asymptotic behavior of the sampling SEP at a high SNR can be presented in terms of diversity order and coding gain. Consider parameters $K_a = a^2/2 + mN_s/\Omega$ and $K_{ab} = (a^2 + b^2)/2 + mN_s/\Omega$ in the earlier expressions. Symbols a^2 and b^2 are the received SNR over the in-phase and quadrature channels, respectively. The symbol Ω is the average fading power and is equal to the unity when the average received power remains the same with and without fading. Therefore, we can evaluate $K_a \approx a^2/2$ and $K_{ab} \approx (a^2+b^2)/2$ at a high SNR. Now, we find the asymptotical expressions, i.e.,

$$\begin{aligned} &\Psi_{as}(a,\, m,\, N_s,\, N_d) \\ &= \frac{N_s}{2\sqrt{\pi mN_sN_d}}\left(1-\exp\left\{-c_o\sqrt{2mN_sN_d}\right\}\right)\frac{\Gamma(mN_sN_d)}{\Gamma(mN_d)^{N_s}} \\ &\quad \times \left(\frac{2m}{\Omega}\right)^{mN_sN_d}(mN_d)^{-(N_s-1)}(a^2)^{-mN_sN_d} \end{aligned} \quad (22)$$

$$\begin{aligned} &\Upsilon_{as}(a,\, b,\, m,\, N_s,\, N_d) \\ &= \frac{N_s(\gamma+\gamma^{-1})}{4\pi mN_sN_d}\left(1-\exp\left\{-c_o\sqrt{\frac{2mN_sN_d}{1+\gamma^2}}\right\}\right) \\ &\quad \times \left(1-\exp\left\{-c_o\sqrt{\frac{2mN_sN_d}{1+\gamma^{-2}}}\right\}\right)\left(\frac{2m}{\Omega(1+\gamma^2)}\right)^{mN_sN_d} \\ &\quad \times \frac{\Gamma(mN_sN_d)}{\Gamma(mN_d)^{N_s}}(mN_d)^{-(N_s-1)}(a^2)^{-mN_sN_d}. \end{aligned} \quad (23)$$

For $M_I = M_Q = \sqrt{M}$, the sampling SEP of general-order rectangular QAM in MIMO with TAS/MRC gracefully reduces to that of square M-QAM. The performance of an uncoded MIMO with TAS/MRC has been investigated for square M-QAM in independent flat Nakagami-m fading channels with N_s transmit and N_d receive antennas. The exact SEP expression was obtained based on the MGF method for square M-QAM with the constellation size M as [6, eq. (36)]

$$\begin{aligned} P_M &= \frac{4}{\pi}\left(1-\frac{1}{\sqrt{M}}\right)\int_0^{\frac{\pi}{2}} M_\gamma\left(-\frac{3}{2(M-1)\sin^2\theta}\right)d\theta \\ &\quad -\frac{4}{\pi}\left(1-\frac{1}{\sqrt{M}}\right)^2\int_0^{\frac{\pi}{4}} M_\gamma\left(-\frac{3}{2(M-1)\sin^2\theta}\right)d\theta \end{aligned} \quad (24)$$

where $M_\gamma(\cdot)$ indicates the MGF associated with the instantaneous postprocessing SNR of TAS/MRC in a MIMO system. The resultant SEP of square M-QAM is shown in [6, eq. (39)] and repeated in the following to compare the computational complexity to the sampling SEP in (20) and (21):

$$\begin{aligned}P_M =& 4\left(1-\frac{1}{\sqrt{M}}\right)\frac{N_s}{[\Gamma(mN_d)]^{N_s}}\\ &\times\sum_{n_1=0}^{+\infty}\sum_{n_2=0}^{+\infty}\cdots\sum_{n_{N_s-1}=0}^{+\infty}\\ &\times\prod_{i=1}^{N_s-1}\frac{(-1)^{n_i}}{n_i!(mN_d+n_i)}\Gamma\left(mN_sN_d+\sum_{k=1}^{N_s-1}n_k\right)\\ &\times\left\{\frac{\left[1+\frac{3\bar{\gamma}}{2m(M-1)}\right]^{-\left(mN_sN_d+\sum_{k=1}^{N_s-1}n_k\right)}}{2\sqrt{\pi}}\right.\\ &\quad\times\frac{\Gamma\left(mN_sN_d+\sum_{k=1}^{N_s-1}n_k+\frac{1}{2}\right)}{\Gamma\left(mN_sN_d+\sum_{k=1}^{N_s-1}n_k+1\right)}\\ &\quad\times{}_2F_1\left(mN_sN_d+\sum_{k=1}^{N_s-1}n_k,\frac{1}{2};mN_sN_d\right.\\ &\qquad\left.+\sum_{k=1}^{N_s-1}n_k+1;\frac{1}{1+\frac{3\bar{\gamma}}{2m(M-1)}}\right)\\ &\quad-\left(1-\frac{1}{\sqrt{M}}\right)\frac{\left[1+\frac{3\bar{\gamma}}{m(M-1)}\right]^{-\left(mN_sN_d+\sum_{k=1}^{N_s-1}n_k\right)}}{2\pi\left[2\left(mN_sN_d+\sum_{k=1}^{N_s-1}n_k\right)+1\right]}\\ &\quad\times F_1\left(1,mN_sN_d+\sum_{k=1}^{N_s-1}n_k,1;mN_sN_d\right.\\ &\qquad\left.\left.+\sum_{k=1}^{N_s-1}n_k+\frac{3}{2};\frac{1+\frac{3\bar{\gamma}}{2m(M-1)}}{1+\frac{3\bar{\gamma}}{m(M-1)}},\frac{1}{2}\right)\right\}\end{aligned}\tag{25}$$

where $\bar{\gamma}$ is the average SNR at the receiver in (15). We can notice that the sampling SEP shows much simpler expression by eliminating the hypergeometric functions $F_1(\cdot)$ and ${}_2F_1(\cdot)$ [18], [19] from the solution.

With $n_1=n_2=\cdots n_{N_s-1}=0$ in (25), the corresponding asymptotic SEP expression is also presented in [6, eq. (40)] and is shown in the following:

$$\begin{aligned}P_M^{\text{asymp}}&=2\left(1-\frac{1}{\sqrt{M}}\right)\frac{\Gamma(mN_sN_d+1)}{[\Gamma(mN_d+1)]^{N_s}}\left[\frac{3}{m(M-1)}\right]^{-mN_sN_d}\\ &\quad\times\left\{\frac{2^{mN_sN_d}}{\sqrt{\pi}}\frac{\Gamma(mN_sN_d+\frac{1}{2})}{\Gamma(mN_sN_d+1)}\right.\\ &\qquad\left.-\frac{\left(1-\frac{1}{\sqrt{M}}\right)F_1(1,mN_sN_d,1;mN_sN_d+\frac{3}{2};\frac{1}{2},\frac{1}{2})}{(2mN_sN_d+1)\pi}\right\}\\ &\quad\times\bar{\gamma}^{-mN_sN_d}+o\left(\bar{\gamma}^{-mN_sN_d}\right)\end{aligned}\tag{26}$$

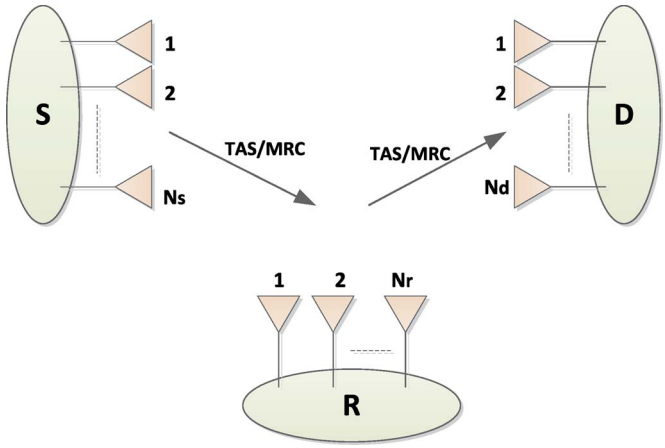

Fig. 2. MIMO relay networks with distributed TAS/MRC. Source (S), relay (R), and destination (D).

which indicates an asymptotic diversity order of mN_sN_d. This result can be compared with the asymptotic sampling SEP in (22) and (23). We find that the asymptotic sampling SEP exhibits a much simpler form by eliminating the hypergeometric function $F_1(\cdot)$ from the solution. We can see that both asymptotic sampling SEP and asymptotic SEP in (26) display the identical diversity order of mN_sN_d. One advantage of the sampling SEP is that the coding gain and diversity order are straightforward since only the last factor $(a^2)^{-mN_sN_d}$ in (22) and (23) contains the in-phase SNR. However, the asymptotic SEP in (26) includes the remainder term of $o(\bar{\gamma}^{-mN_sN_d})$ that is not explicitly specified. The behavior of the asymptotic SEP largely depends on how fast the remainder term vanishes as the SNR increases. An additional benefit of the sampling SEP is that the effect of system parameters, such as fading and the number of antennas in the transmitter, relay and receiver, is transparent in the sampling SEP. On the other hand, the function of system parameters is hidden in the hypergeometric functions in the conventional SEP.

IV. Sampling Symbol Error Probablity in Multiple-Input–Multiple-Output Relay Networks With Distributed Transmit Antenna Selection/Maximal Ratio Combining

Let us consider the SEP of distributed TAS/MRC in MIMO relay networks shown in Fig. 2. A full MIMO system is realized with N_s, N_r, and N_d antennas at the source, relay, and destination, respectively.

The SEP in amplify-and-forward MIMO relay can be approximated at a high SNR as [2], [20]

$$P^{\text{relay}}\approx P^1+P^2\tag{27}$$

where P^1 and P^2 are the SEP at the first and second hops, respectively. Therefore, the sampling SEP of the general-order rectangular $M_I\times M_Q$-QAM in the MIMO relay with TAS/MRC can be attained as

$$\begin{aligned}&P_s^{\text{relay}}(a_1,b_1,a_2,b_2,m_1,m_2,N_s,N_r,N_d)\\ &\quad=P_s(a_1,b_1,m_1,N_s,N_r)+P_s(a_2,b_2,m_2,N_r,N_d)\end{aligned}\tag{28}$$

where P_s is the sampling SEP in each hop. Symbols m_1 and m_2 indicate fading parameters in the first hop (source to relay) and the second hop (relay to destination), respectively. Likewise, a_i and b_i are general-order rectangular QAM constellation parameters in the ith hop. The sampling SEP in (28) is in closed form, and fading parameters can be arbitrary real values. We can see that the diversity order is $\min(m_1 N_s N_r,\, m_2 N_r N_d)$, which is the diversity order of the weakest hop that causes the dominant error in overall path.

For $M_I = M_Q = \sqrt{M}$, the sampling SEP of general-order rectangular QAM reduces to that of square M-QAM. In the context of TAS/MRC in a full MIMO design, the exact SEP of a square M-QAM modulation can be expressed as in (24), replacing the MGF $M_\gamma(\cdot)$ with $M_{\gamma_{\rm eq}}(\cdot)$ defined in [7, eq. (13)], which is the MGF of the equivalent instantaneous end-to-end SNR of distributed TAS/MRC in MIMO relay networks. The equivalent instantaneous SNR $\gamma_{\rm eq}$ for amplify-and-forward relay can be represented as [7, eq. (4)] [20]

$$\gamma_{\rm eq} = \frac{\gamma_1 \gamma_2}{\gamma_1 + \gamma_2} \tag{29}$$

where γ_1 is the instantaneous received SNR after performing MRC at the relay, and γ_2 is the instantaneous received SNR from the relay after performing MRC at the destination. Note that the symbols γ_i are unrelated to the ratio of the quadrature to in-phase decision distance of γ in Section III. The exact SEP of the square M-QAM should be numerically evaluated from (24) using MGF $M_{\gamma_{\rm eq}}(\cdot)$. We repeat the MGF to compare the computational complexity to the sampling SEP, as shown in (30) [7] at the bottom of the page, where m_1 and m_2 are integer-valued fading parameter in the first hop and the second hop, respectively. Remember that the fading parameters in the sampling SEP can be any real values. The symbols $\bar{\gamma}_1$ and $\bar{\gamma}_2$ are the average received SNR after performing MRC at the relay and the destination, respectively. We find that the exact SEP of square M-QAM is time-consuming to numerically evaluate, particularly at high SNR due to the increased number of terms to be added in the Gauss hypergeometric function in the MGF to ensure the convergence. We can see that key system parameters are buried in the hypergeometric function in the SEP and can hardly capture their effects on the system performance. On the other hand, the function of system parameters in the sampling SEP is transparent. The transparency of key parameters of the MIMO system in its performance evaluation is crucial for system design, validation, and industrial standardization processes.

The corresponding asymptotic SEP of square M-QAM is derived using a first-order Taylor series expansion of $M_{\gamma_{\rm eq}}(\cdot)$ as $\gamma_1 \to \infty$ shown in the following [7]:

$$\begin{aligned} P_M^{\rm relay,\,asymp} &= \frac{2\Phi}{\pi}\left(1-\frac{1}{\sqrt{M}}\right)\left(\frac{2(M-1)}{3}\right)^q \\ &\quad\times\left[\sqrt{\pi}\Gamma\left(\frac{1}{2}+q\right)-\Gamma(1+q)\left(1-\frac{1}{\sqrt{M}}\right)\right. \\ &\quad\left.\times B_{\frac{1}{2}}\left(\frac{1}{2}+q,\frac{1}{2}\right)\right]\bar{\gamma}_1^{-q}+o(\bar{\gamma}_1^{-q}) \end{aligned} \tag{31}$$

where $B_z(a,\,b)=\int_0^z t^{a-1}(1-t)^{b-1}dt$ is the incomplete beta function. $q = N_r \times \min(m_1 N_s,\, m_2 N_d)$ is a diversity order of TAS/MRC in the MIMO relay network. The symbol Φ[1] is defined in

$$\Phi = \left\{ \begin{array}{ll} \frac{m_1^{m_1 N_s N_r}}{(m_1 N_r)!^{N_s}}, & \text{when } \; m_1 N_s < m_2 N_d \\ \frac{m_2^{m_2 N_r N_d}}{\rho^q (m_2 N_d)!^{N_r}}, & \text{when } \; m_1 N_s > m_2 N_d \\ \frac{m_1^{m_1 N_s N_r}}{(m_1 N_r)!^{N_s}} + \frac{m_2^{m_2 N_r N_d}}{\rho^q (m_2 N_d)!^{N_r}}, & \text{when } \; m_1 N_s = m_2 N_d \end{array} \right\} \tag{32}$$

[1]Note that [7, Eq. (17)] has apparent typographical errors. In [7, Eq. (17)] $N_S < N_D$, $N_S > N_D$ and $N_S = N_D$ should be $m_1 N_S < m_2 N_D$, $m_1 N_S > m_2 N_D$, and $m_1 N_S = m_2 N_D$, respectively.

$$\begin{aligned} M_{\gamma_{\rm eq}}(s) &= 1 + s\frac{N_r\sqrt{\pi}}{\Gamma(m_2 N_d)} \sum_{q_0=1}^{N_s}\sum_{r_0=0}^{N_r-1}\binom{N_s}{q_0}\binom{N_r-1}{r_0}(-1)^{q_0+r_0-1} \prod_{k=1}^{m_1 N_r-1}\left[\sum_{q_k=0}^{q_{k-1}}\binom{q_{k-1}}{q_k}\left(\frac{1}{k!}\right)^{q_k-q_{k+1}}\right] \\ &\quad\times \prod_{l=1}^{m_2 N_d-1}\left[\sum_{r_l=0}^{r_{l-1}}\binom{r_{l-1}}{r_l}\left(\frac{1}{l!}\right)^{r_l-r_{l+1}}\right] \sum_{i=0}^{\sigma}\sum_{j=0}^{\zeta+m_2N_d-1}\binom{\sigma}{i}\binom{\zeta+m_2N_d-1}{j}\left(\frac{m_2}{\bar{\gamma}_2}\right)^{\zeta+m_2N_d-j+i-1}\left(\frac{m_1}{\bar{\gamma}_1}\right)^{\sigma} \\ &\quad\times (r_0+1)^{i-j-1}\left(\frac{q_0 m_1}{\bar{\gamma}_1}+\frac{(r_0+1)m_2}{\bar{\gamma}_2}-s\right)^{j-i-\sigma-\zeta-m_2N_d} 2^{-\sigma-\zeta-m_2N_d-j+i-1} \\ &\quad\times \frac{\Gamma(\sigma+\zeta+m_2N_d-j+i)\Gamma(\sigma+\zeta+m_2N_d+j-i+2)}{\Gamma\left(\sigma+\zeta+m_2N_d+\frac{3}{2}\right)}{}_2F_1 \\ &\quad\times\left[\frac{\sigma+\zeta+m_2N_d-j+i}{2},\frac{\sigma+\zeta+m_2N_d-j+i+1}{2};\sigma+\zeta+m_2N_d\right. \\ &\qquad\left.+\frac{3}{2};1-\frac{4q_0(r_0+1)m_1m_2}{\bar{\gamma}_1\bar{\gamma}_2}\left(\frac{q_0m_1}{\bar{\gamma}_1}+\frac{(r_0+1)m_2}{\bar{\gamma}_2}-s\right)^{-2}\right] \end{aligned} \tag{30}$$

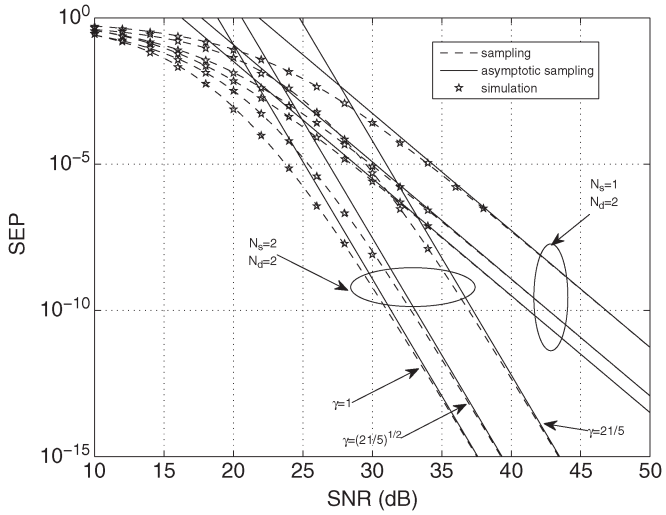

Fig. 3. Simulation and sampling SEP. 8 × 4-QAM, MIMO, TAS/MRC. $\gamma = 1, (21/5)^{1/2}, 21/5$; Nakagami-$m$ fading, $m = 2$; $N_s = 1, 2$; and $N_d = 2$.

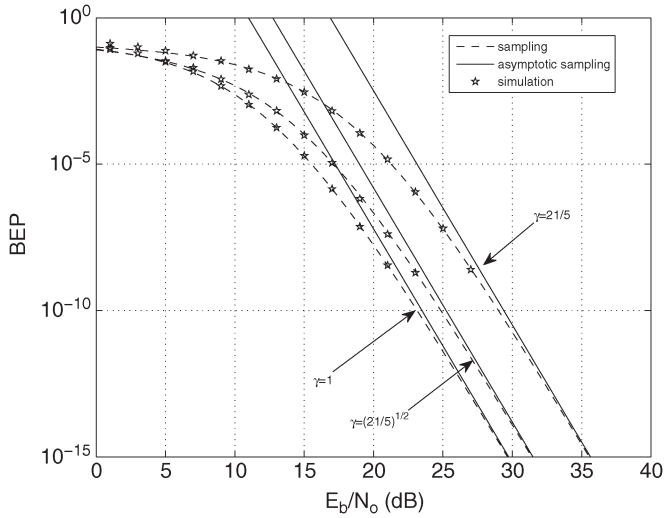

Fig. 4. Simulation and sampling BEP with Gray code. 8 × 4-QAM, MIMO, TAS/MRC. $\gamma = 1, (21/5)^{1/2}, 21/5$; Nakagami-$m$ fading, $m = 2$; $N_s = 2$; and $N_d = 2$.

where $\rho = \bar{\gamma}_2/\bar{\gamma}_1$ is the ratio of the per-hop average received SNRs. The symbol q is defined as $q = N_r \times \min(m_1 N_s,\ m_2 N_d)$. Notice that the fading parameters in the asymptotic SEP in (32) should be also integer values, whereas those of the asymptotic sampling SEP can be any arbitrary real values. In addition, the asymptotic sampling SEP does not contain the remainder term, such as $o(\bar{\gamma}_1^{-q})$ in (31). The enormous computational complexity involved in (25) and (30) for MIMO and MIMO relay networks, respectively, hinders our attempts to find the exact SEP of square M-QAM. Even asymptotic SEPs are much more complicated than the corresponding asymptotic sampling SEPs. Most importantly, to establish a feasible MGF for an integration with an alternative form of the Q-function [21], [22, Eq. (4.2)], [23], the corresponding overall fading pdf should be in a suitable form eventually to obtain the SEP. These are partly the reason that the performance of general-order rectangular QAM is not available in literature for MIMO relay networks with TAS/MRC in Nakagami-m fading channels in spite of its practical usefulness. However, the sampling property of the delta impulse function can be easily applied to obtain the sampling SEP without MGF at all.

V. Numerical Results

We first examine the MIMO with TAS/MRC in Fig. 1 to obtain the simulated and analytical results. The sampling SEP of the rectangular 8 × 4-QAM is compared with the simulation SEP in Fig. 3 for $m = 2$, $N_s = 1, 2$, and $N_d = 2$. The values of $\gamma = 1$ and $\gamma = (21/5)^{1/2}$ indicate an equal decision distance and equal signal energy (for in-phase and quadrature), respectively. We can see that the sampling SEP accurately represents the simulation SEP for all values of γ. In addition, the asymptotic sampling SEP illustrates well the behavior of the simulation SEP at a high SNR. The BEP of the 8 × 4-QAM is shown in Fig. 4 with $N_s = N_d = 2$ and fading parameter $m = 2$. The Gray code is employed to minimize the BEP per symbol error. The analytical BEP is obtained by dividing the SEP by the number of bits per symbol, which is 5 in this case.

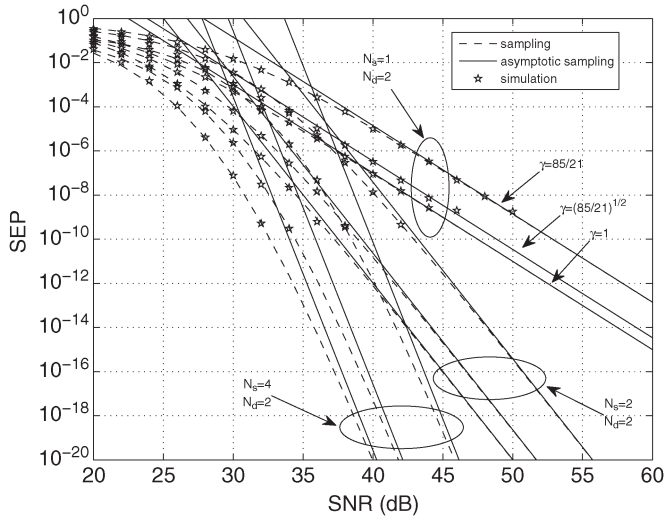

Fig. 5. Simulation and sampling SEP. 16 × 8-QAM, MIMO, TAS/MRC. $\gamma = 1, (85/21)^{1/2}, 85/21$; Nakagami-$m$ fading, $m = 2$; $N_s = 1, 2, 4$; and $N_d = 2$.

Most likely, symbol error occurs when the received symbol is mistaken by the nearest symbol, which causes one bit error due to the Gray code implemented in the system. Both sampling and asymptotic sampling BEPs accurately reflect the simulation result.

In Fig. 5, the simulation SEP and sampling SEP of 16 × 8-QAM are shown for the number of transmit antennas $N_s = 1, 2, 4$, the number of receive antennas $N_d = 2$, and the fading parameter $m = 2$. For all different numbers of transmit antennas, the equal decision distance $\gamma = 1$ case displays the best performance as we expected. The performance improvement from $N_s = 1$ to $N_s = 2$ is more significant than the improvement from $N_s = 2$ to $N_s = 4$. Therefore, we can see that the performance improvement step decreases as the number of transmit antennas increases. For all transmit and receive antenna pairs, the diversity order and coding gain faithfully portray the sampling SEP at a high SNR.

The sampling SEP for general-order rectangular $M_I \times M_Q$-QAM reduces to square M-QAM for $M_I = M_Q = \sqrt{M}$.

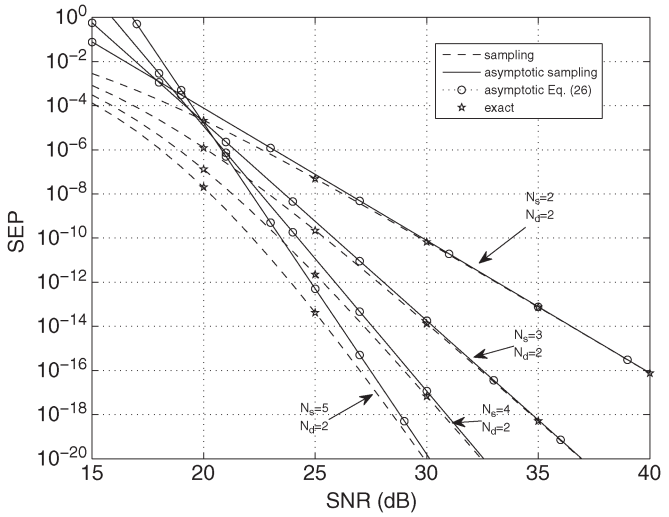

Fig. 6. Exact and sampling SEP. 16-QAM, MIMO, TAS/MRC. Nakagami-m fading, $m = 1.5$; $N_s = 2, 3, 4, 5$; and $N_d = 2$.

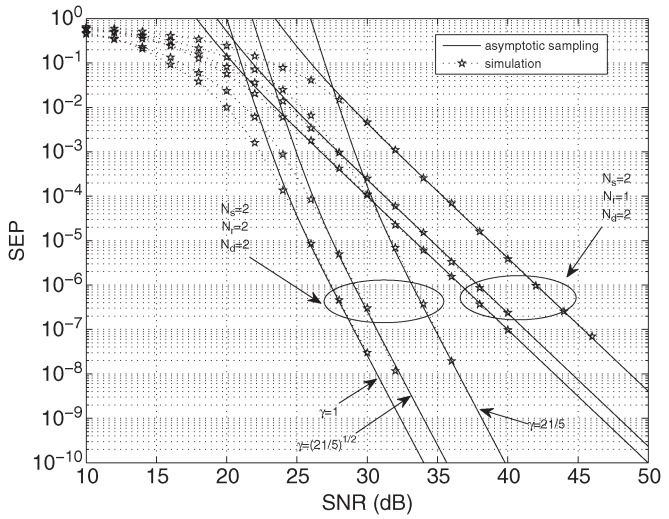

Fig. 7. Simulation and sampling SEP. 8 × 4-QAM, MIMO relay networks, TAS/MRC. $\gamma = 1$, $(21/5)^{1/2}$, 21/5; Nakagami-m fading, $m_1 = 1.5$, $m_2 = 2.5$; $N_s = 2$; $N_r = 1, 2$; and $N_d = 2$.

We consider the square 16-QAM MIMO with TAS/MRC in Fig. 6 for $m = 1.5$, $N_s = 2, 3, 4, 5$, and $N_d = 2$. The sampling SEP and asymptotic sampling SEP are compared with the exact and asymptotic SEP, respectively. We can see that the sampling SEP represents the exact SEP accurately for all SNR. In addition, the asymptotic sampling SEP precisely overlaps with the conventional asymptotic SEP in (26) for all SNR. Therefore, we can see that the sampling SEP provides an accurate performance evaluation with a remarkably simple expression and significantly reduced computational complexity.

Now, we examine MIMO relay networks in Fig. 2 with the same average received SNR at the relay and destination. The asymptotic sampling SEP of the rectangular 8 × 4-QAM relay networks is compared with the simulation SEP in Fig. 7 for the fading parameter per hop, $m_1 = 1.5$, $m_2 = 2.5$, and the number of antennas, $N_s = 2$, $N_r = 1, 2$, and $N_d = 2$. We can see that the asymptotic sampling SEP approaches the simulation SEP at a moderate or high SNR, where the actual operating point

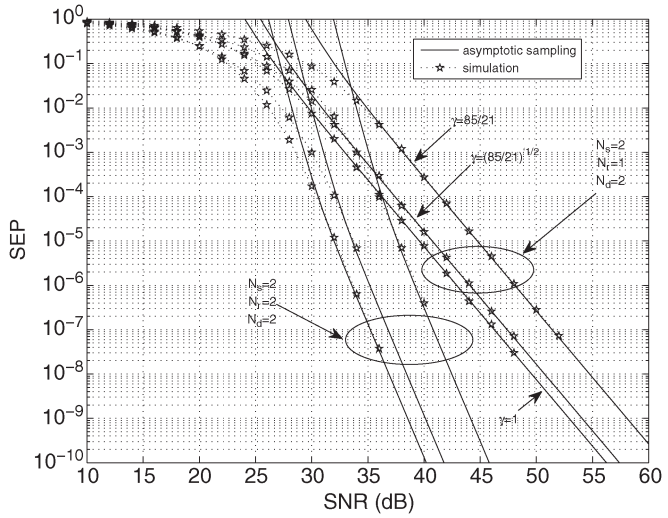

Fig. 8. Simulation and sampling SEP. 16 × 8-QAM, MIMO relay networks, TAS/MRC. $\gamma = 1$, $(85/21)^{1/2}$, 85/21; Nakagami-m fading, $m_1 = 1.5$, $m_2 = 2.5$; $N_s = 2$; $N_r = 1, 2$; and $N_d = 2$.

is located in practice. In fact, the asymptotic sampling SEP portrays well the simulation SEP at a high SNR for different numbers of relay antennas. The performance enhancement with the diversity order is apparent. Regardless of the number of antennas at the source, relay and destination, the equal decision distance $\gamma = 1$ case exhibits the best performance as we expected.

Fig. 8 displays the simulation and asymptotic sampling SEP of 16 × 8-QAM relay in the same scenario of Fig. 7. The performance degradation due to the increased constellation size is apparent. For example, with $N_s = 2$, $N_r = 1$, and $N_d = 2$, the SEP of 10^{-6} is achieved at the SNR of 38 dB with the equal signal energy $\gamma = (21/5)^{1/2}$ for 8 × 4-QAM. However, with the same parameters, the same SEP is achieved for 16 × 8-QAM at the SNR of 44 dB with $\gamma = (85/21)^{1/2}$. Therefore, the signal power needs to be quadrupled to achieve the same performance for the increased constellation size with given system parameters. The asymptotic sampling SEP depicts the simulation SEP closely at a high SNR. We observed that the sampling SEP somewhat diverges from the actual SEP at a low SNR due to the performance approximation of relay networks in (27), as noted earlier.

Channel coding is employed to the MIMO with 8 × 4-QAM with $N_s = N_d = 2$ in Fig. 9. The convolutional coding with the code rate $R = 1/2$ and the generator matrix $G = [5, 7]$ in octal applied to the rectangular QAM with Gray code. The channel coding gain is incorporated to the analytical result. Still, the asymptotic sampling BEP accurately represents simulation results at moderate and high SNRs. The simple convolutional coding with the code rate of 1/2 shifts the BEP curve to the low SNR region. A significantly larger channel coding gain with Turbo code or low-density parity-check code, which has been adopted in wireless communication standards, obviously can move the BEP curve to a much lower SNR region.

For $M_I = M_Q = \sqrt{M}$, the sampling SEP of general-order rectangular QAM gracefully reduces to that of square QAM. The exact and asymptotic sampling SEPs are shown in Fig. 10

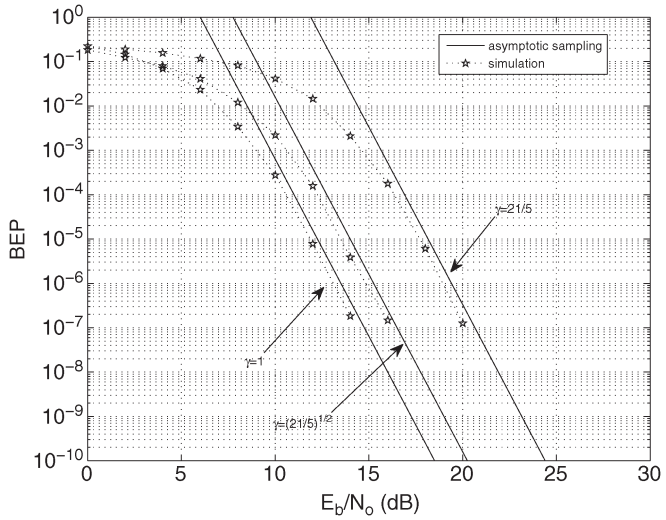

Fig. 9. Simulation and sampling BEP with Gray code. Convolutional coding with $R = 1/2$ and $G = [5, 7]$. 8 $\times$ 4-QAM, MIMO, TAS/MRC. $\gamma = 1$, $(21/5)^{1/2}$, 21/5; Nakagami-m fading, $m = 2$; $N_s = 2$; and $N_d = 2$.

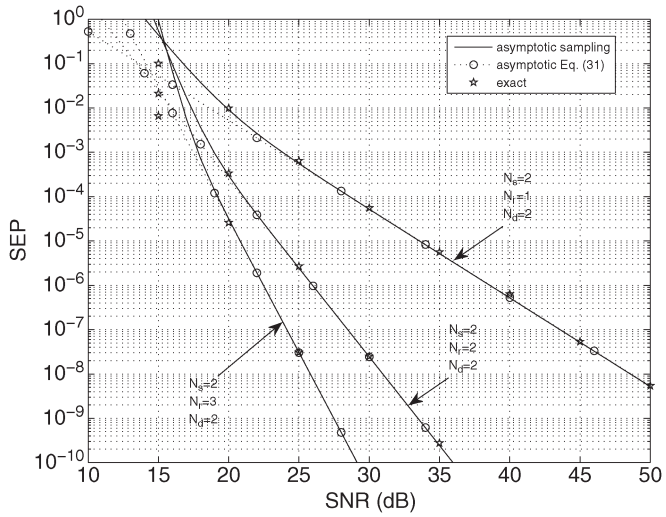

Fig. 10. Exact and sampling SEP. 16-QAM, MIMO relay networks, TAS/MRC. Nakagami-m fading, $m_1 = 2$, $m_2 = 1$; $N_s = 2$; $N_r = 1, 2, 3$; and $N_d = 2$.

for the square 16-QAM. We employ fading parameters in each hop, i.e., $m_1 = 2$ and $m_2 = 1$, and the number of source, relay, and destination antennas, i.e., $N_s = 2$, $N_r = 1, 2, 3$, and $N_d = 2$, respectively. Here, we chose integer fading parameters to compare the sampling SEP to the exact and asymptotic SEP in (30) and (31) [7], respectively. We can see that the asymptotic sampling SEP accurately represents the exact SEP at moderate and high SNRs. The asymptotic sampling SEP overlaps the conventional asymptotic SEP in (31) at a moderate and high SNR. In fact, the asymptotic sampling SEP coincides with the exact SEP at the SNR up to 20 dB for the number of relay antennas $N_r = 1$ and 2, whereas the asymptotic SEP in (31) starts to deviate from the exact SEP. The exact SEP was numerically computed from (24) using the MGF in (30). It took 6 h to evaluate numerically the exact SEP at the SNR equal to 30 dB for $N_s = 2$, $N_r = 3$, and $N_d = 2$ using MATLAB Version 7.12 on a Dell Precision 390 workstation, although the code can be optimized. However, the sampling SEP can be obtained in a second for the same parameters.

The sampling SEP can be easily extended to multihop MIMO relaying or MIMO with cooperative diversity [2]. We noticed that the sampling SEP tends to somewhat deviate from the actual SEP as the diversity order increases. A similar effect can be observed in other simple approaches for quantifying system performance [20], [24]. However, the sampling method can accurately predict the exact performance of the system with practical diversity order.

VI. Conclusion

We have obtained the SEP of general-order rectangular QAM in MIMO with TAS/MRC in Nakagami-m fading channels using sampling. The sampling SEP is very simple, accurate, and easy to understand the effect of each system parameters on the performance, such as fading or the number of antennas at the source, relay, and destination. The sampling SEP of MIMO coincides with the simulation SEP for all SNRs with different system parameters, including real or integer fading parameters. The sampling SEP is extended to MIMO relay networks in terms of coding gain and diversity order. The asymptotic sampling SEP portrays the simulation SEP faithfully at moderate and high SNRs with a practical diversity order. The results are crucial to understanding the system performance of general-order rectangular QAM in MIMO relay networks since the exact SEP is not available in literature in spite of the recent ample interest from both industry and academia. The proposed sampling SEP of general-order QAM gracefully reduces to that of square QAM. The sampling SEP is verified with the exact SEP of square M-QAM currently available in literature.

Appendix
Sampling Performance

For MIMO with N_s transmit and N_d receive antennas in independent flat Nakagami-m fading channels, $\Psi(\cdot)$ in (17) can be rewritten for sampling using the Q-function approximation $Q(x) \approx (1/\sqrt{2\pi}x)(1 - \exp\{-c_o x\})\exp\{-x^2/2\}$ with $c_o = \sqrt{\pi/2}$ as [25]

$$\begin{aligned}\Psi_s(a,\, m,\, N_s,\, N_d) &= \int_0^\infty \frac{1}{\sqrt{2\pi}ar}\left(1 - \exp\{-c_o ar\}\right) \\ &\quad \times \exp\left\{-\frac{a^2}{2}r^2\right\} 2N_s \left(\frac{m}{\Omega}\right)^{mN_d} \frac{r^{2mN_d-1}}{\Gamma(mN_d)} \\ &\quad \times \exp\left\{-\frac{m}{\Omega}r^2\right\}\left[\frac{\gamma(mN_d,\, \frac{m}{\Omega}r^2}{\Gamma(mN_d)}\right]^{N_s-1} dr \end{aligned} \quad (33)$$

where the lower incomplete gamma function can be expressed as [18, eq. (3.381)]

$$\gamma(\alpha,\, x) = \exp\{-x\}\sum_{k=0}^{\infty} \frac{x^{\alpha+k}}{\alpha(\alpha+1)\cdots(\alpha+k)}. \quad (34)$$

Therefore

$$\left[\frac{\gamma(mN_d, \frac{m}{\Omega}r^2)}{\Gamma(mN_d)}\right]^{N_s-1} = \left[\frac{\exp\{-\frac{m}{\Omega}r^2\}}{\Gamma(mN_d)}\sum_{k=0}^{\infty}\frac{\left(\frac{m}{\Omega}r^2\right)^{mN_d+k}}{\prod_{i=0}^{k}(mN_d+i)}\right]^{N_s-1} \tag{35}$$

$$= \frac{\exp\left\{-(\frac{m}{\Omega}r^2)(N_s-1)\right\}}{\Gamma(mN_d)^{N_s-1}}\left(\frac{m}{\Omega}r^2\right)^{mN_d(N_s-1)} \times\left[\sum_{k=0}^{\infty}\frac{\left(\frac{m}{\Omega}r^2\right)^{k}}{\prod_{i=0}^{k}(mN_d+i)}\right]^{N_s-1} \tag{36}$$

and (33) can be written as

$$\Psi_s(a,\, m,\, N_s,\, N_d) = \int_0^{\infty}\frac{1}{\sqrt{2\pi}ar}\left(1-\exp\{-c_o ar\}\right) \times\exp\left\{-\frac{a^2}{2}r^2\right\}2N_s\left(\frac{m}{\Omega}\right)^{mN_d}\frac{r^{2mN_d-1}}{\Gamma(mN_d)} \times\exp\left\{-\frac{m}{\Omega}r^2\right\}\frac{\exp\left\{-\left(\frac{m}{\Omega}r^2\right)(N_s-1)\right\}}{\Gamma(mN_d)^{N_s-1}} \times\left(\frac{m}{\Omega}r^2\right)^{mN_d(N_s-1)}\left[\sum_{k=0}^{\infty}\frac{\left(\frac{m}{\Omega}r^2\right)^{k}}{\prod_{i=0}^{k}(mN_d+i)}\right]^{N_s-1} dr. \tag{37}$$

If we choose preimpulse function

$$g_p(r) = r^{2mN_d-1}r^{2mN_d(N_s-1)}\exp\left\{-\frac{a^2}{2}r^2\right\} \times\exp\left\{-\frac{mN_s}{\Omega}r^2\right\} \tag{38}$$

$$= r^{2mN_sN_d-1}\exp\{-K_a r^2\} \tag{39}$$

with $K_a = a^2/2 + mN_s/\Omega$, we can obtain the asymptotic impulse function as [1]

$$g(r) = \frac{1}{2}\frac{\Gamma(mN_sN_d)}{K_a^{mN_sN_d}}\delta\left(r-\sqrt{\frac{mN_sN_d}{K_a}}\right). \tag{40}$$

Then, (37) can be rewritten as

$$\Psi_s(a,\, m,\, N_s,\, N_d) = \int_0^{\infty}\frac{1}{\sqrt{2\pi}ar}\left(1-\exp\{-c_o ar\}\right)\frac{2N_s}{\Gamma(mN_d)^{N_s}}\left(\frac{m}{\Omega}\right)^{mN_dN_s} \times\left[\sum_{k=0}^{\infty}\frac{\left(\frac{m}{\Omega}r^2\right)^{k}}{\prod_{i=0}^{k}(mN_d+i)}\right]^{N_s-1} \times\frac{1}{2}\frac{\Gamma(mN_sN_d)}{K_a^{mN_sN_d}}\delta\left(r-\sqrt{\frac{mN_sN_d}{K_a}}\right)dr \tag{41}$$

and the sampling result is shown in (20).

In a similar way, $\Upsilon(\cdot)$ in (18) can be rewritten for sampling as

$$\Upsilon_s(a,\, b,\, m,\, N_s,\, N_d) = \int_0^{\infty}\frac{1}{\sqrt{2\pi}ar}\left(1-\exp\{-c_o ar\}\right) \times\exp\left\{-\frac{a^2}{2}r^2\right\}\frac{1}{\sqrt{2\pi}br}\left(1-\exp\{-c_o br\}\right) \times\exp\left\{-\frac{b^2}{2}r^2\right\}2N_s\left(\frac{m}{\Omega}\right)^{mN_d}\frac{r^{2mN_d-1}}{\Gamma(mN_d)} \times\exp\left\{-\frac{m}{\Omega}r^2\right\}\left[\frac{\gamma(mN_d, \frac{m}{\Omega}r^2)}{\Gamma(mN_d)}\right]^{N_s-1} dr \tag{42}$$

$$= \int_0^{\infty}\frac{1}{\sqrt{2\pi}ar}\left(1-\exp\{-c_o ar\}\right) \times\exp\left\{-\frac{a^2}{2}r^2\right\}\frac{1}{\sqrt{2\pi}br}\left(1-\exp\{-c_o br\}\right) \times\exp\left\{-\frac{b^2}{2}r^2\right\}2N_s\left(\frac{m}{\Omega}\right)^{mN_d}\frac{r^{2mN_d-1}}{\Gamma(mN_d)} \times\exp\left\{-\frac{m}{\Omega}r^2\right\}\frac{\exp\left\{-\left(\frac{m}{\Omega}r^2\right)(N_s-1)\right\}}{\Gamma(mN_d)^{N_s-1}} \times\left(\frac{m}{\Omega}r^2\right)^{mN_d(N_s-1)}\left[\sum_{k=0}^{\infty}\frac{\left(\frac{m}{\Omega}r^2\right)^{k}}{\prod_{i=0}^{k}(mN_d+i)}\right]^{N_s-1} dr. \tag{43}$$

If we choose preimpulse function

$$g_p(r) = r^{2mN_d-1}r^{2mN_d(N_s-1)}\exp\left\{-\frac{a^2}{2}r^2\right\} \times\exp\left\{-\frac{b^2}{2}r^2\right\}\exp\left\{-\frac{mN_s}{\Omega}r^2\right\} \tag{44}$$

$$= r^{2mN_sN_d-1}\exp\{-K_{ab}r^2\} \tag{45}$$

with $K_{ab} = (a^2+b^2)/2 + mN_s/\Omega$, we can obtain the asymptotic impulse function as

$$g(r) = \frac{1}{2}\frac{\Gamma(mN_sN_d)}{K_{ab}^{mN_sN_d}}\delta\left(r-\sqrt{\frac{mN_sN_d}{K_{ab}}}\right). \tag{46}$$

Then, (43) can be expressed as

$$\Upsilon_s(a,\, b,\, m,\, N_s,\, N_d) = \int_0^{\infty}\frac{1}{2\pi abr^2}\left(1-\exp\{-c_o ar\}\right)\left(1-\exp\{-c_o br\}\right) \times\left(\frac{m}{\Omega}\right)^{mN_d}\frac{2N_s}{\Gamma(mN_d)}\frac{\left(\frac{m}{\Omega}\right)^{mN_d(N_s-1)}}{\Gamma(mN_d)^{N_s-1}} \times\left[\sum_{k=0}^{\infty}\frac{\left(\frac{m}{\Omega}r^2\right)^{k}}{\prod_{i=0}^{k}(mN_d+i)}\right]^{N_s-1} \times\frac{1}{2}\frac{\Gamma(mN_sN_d)}{K_{ab}^{mN_sN_d}}\delta\left(r-\sqrt{\frac{mN_sN_d}{K_{ab}}}\right)dr \tag{47}$$

and the sampling result is shown in (21).

REFERENCES

[1] W. M. Jang, "Quantifying performance in fading channels using the sampling property of a delta function," *IEEE Commun. Lett.*, vol. 15, no. 3, pp. 266–268, Mar. 2011.

[2] W. M. Jang, "Quantifying performance of cooperative diversity using the sampling property of a delta function," *IEEE Trans. Wireless Commun.*, vol. 10, no. 7, pp. 2034–2039, Jul. 2011.

[3] W. M. Jang, "A simple performance approximation of general-order rectangular QAM with MRC in Nakagami-m fading channels," *IEEE Trans. Veh. Technol.*, vol. 62, no. 7, pp. 3457–3463, Sep. 2013.

[4] G. K. Karagiannidis, "On the symbol error probability of general order rectangular QAM in Nakagami-m fading," *IEEE Commun. Lett.*, vol. 10, no. 11, pp. 745–747, Nov. 2006.

[5] Z. Chen, J. Yuan, and B. Vucetic, "Analysis of transmit antenna selection/maximal-ratio combining in Rayleigh fading channels," *IEEE Trans. Veh. Technol.*, vol. 54, no. 4, pp. 1312–1321, Jul. 2005.

[6] Z. Chen, Z. Chi, Y. Li, and B. Vucetic, "Error performance of maximal-ratio combining with transmit antenna selection in flat fading Nakagami-m fading channels," *IEEE Trans. Wireless Commun.*, vol. 8, no. 1, pp. 424–431, Jan. 2009.

[7] P. L. Yeoh, M. Elkashlan, and I. B. Collings, "MIMO relaying: Distributed TAS/MRC in Nakagami-m fading," *IEEE Trans. Commun.*, vol. 59, no. 10, pp. 2678–2682, Oct. 2011.

[8] J. M. Romero-Jerez and A. J. Goldsmith, "Performance of multichannel reception with transmit antenna selection in arbitrarily distributed nakagami fading channels," *IEEE Trans. Wireless Commun.*, vol. 8, no. 4, pp. 2006–2013, Apr. 2009.

[9] N. C. Beaulieu, "A useful integral for wireless communication theory and its application to rectangular signaling constellation error rates," *IEEE Trans. Commun.*, vol. 54, no. 5, pp. 802–805, May 2006.

[10] G. Aniba and S. Aissa, "BER evaluation for general QAM in Nakagami-m fading channels," *IET Electron. Lett.*, vol. 45, no. 6, pp. 319–321, Mar. 2009.

[11] R. M. Radaydeh, "Performance analysis of rectangular quadrature amplitude modulation with combined arbitrary transmit antenna selection," *IET Commun.*, vol. 2, no. 8, pp. 1077–1088, Sep. 2008.

[12] W. M. Jang, "Dynamic integration using sampling in fading channels," *IEEE Trans. Commun.*, vol. 60, no. 10, pp. 2768–2775, Oct. 2012.

[13] A. Papoulis and S. U. Pillai, *Probability, Random Variables and Stochastic Processes,* 4th ed. New York, NY, USA: McGraw-Hill, 2002.

[14] J. M. Wozencraft and I. M. Jacobs, *Principles of Communication Engineering*. Hoboken, NJ, USA: Wiley, 1965, p. 83.

[15] J. G. Proakis, *Digital Communications,* 4th ed. New York, NY, USA: McGraw-Hill, 2000.

[16] S. Haykin and M. Moher, *Modern Wireless Communications*. Englewood Cliffs, NJ, USA: Prentice-Hall, 2005, p. 344.

[17] H. A. David, *Order Statistics*. Hoboken, NJ, USA: Wiley, 1970.

[18] I. S. Gradshteyn and I. M. Ryzhik, *Table of Integrals, Series, and Products,* 5th ed. San Diego, CA, USA: Academic, 1994.

[19] H. Exton, *Multiple Hypergeometric Functions and Applications*. Hoboken, NJ: Wiley, 1976.

[20] A. Ribeiro, X. Cai, and G. B. Giannakis, "Symbol error probabilities for general order cooperative links," *IEEE Trans. Wireless Commun.*, vol. 4, no. 3, pp. 1264–1273, May 2005.

[21] M. K. Simon and M.-S. Alouini, "A unified approach to the performance analysis of digital communications over generalized fading channels," *Proc. IEEE*, vol. 86, no. 9, pp. 1860–1877, Sep. 1998.

[22] M. K. Simon and M.-S. Alouini, *Digital Communications Over Fading Channels,* 2nd ed. Hoboken, NJ, USA: Wiley, 2005.

[23] R. Li and P. Y. Kam, "Averages of the product of two Gaussian Q-functions over fading statistics and applications," *IEEE Commun. Lett.*, vol. 11, no. 1, pp. 58–60, Jan. 2007.

[24] Z. Wang and G. B. Giannakis, "A simple and general parameterization quantifying performance in fading channels," *IEEE Trans. Commun.*, vol. 51, no. 8, pp. 1389–1398, Aug. 2003.

[25] W. M. Jang, "A simple upper bound of the Gaussian Q-function with closed-form error bound," *IEEE Commun. Lett.*, vol. 15, no. 2, pp. 157–159, Feb. 2011.

Won Mee Jang received the B.A. degree in computer science from the University of Minnesota, Minneapolis, MN, USA, in 1984; the M.S. degree in computer engineering from George Mason University, Fairfax, VA, USA, in 1987; and the D.Sc. degree in electrical engineering from The George Washington University, Washington, DC, USA, in 1996.

From 1988 to 1991, she was with the Information and Electronics Division, Korea Research Institute of Science and Technology, Pohang, Korea. From 1995 to 1998, she was a Wireless Engineer with Comsearch, Reston, VA, USA. Since 1998, she has been with the Department of Computer and Electronics Engineering, University of Nebraska–Lincoln, Lincoln, NE, USA, where she is currently an Associate Professor. Her research interests include spread spectrum, satellite communications, global navigation satellite systems, code-division multiple access, orthogonal frequency division multiplexing, multiple-input–multiple-output systems, cooperative diversity, cognitive radio, coding, signal modulation/demodulation, and communication theory.